https://doi.org/10.5194/esurf-2021-14
Preprint. Discussion started: 11 March 2021

Earth Surface Dynamics Discussions
Open Access
EGU

Landslide-lake outburst floods accelerate downstream slope slippage

Wentao Yang[1], Jian Fang[2], Jing Liu-Zeng[3]

[1]Three-gorges Reservoir Area (Chongqing) Forest Ecosystem Research Station, School of Soil and Water Conservation, Beijing Forestry University, Beijing, 100083, China
[2]College of Urban and Environmental Sciences, Central China Normal University, Wuhan, 430079, China
[3]Institute of Surface-Earth System Science, Tianjin University, Tianjin, 300072, China

Correspondence to: Wentao Yang (yang_wentao@bjfu.edu.cn)

Abstract. The Jinsha River, carving a 2-4 km deep gorge, is one of the largest SE Asian rivers. Two successive landslide-lake outburst floods (LLFs) occurred after the 2018 Baige landslides along the river. Using Sentinel-2 images, we examined the LLFs' impacts on downstream river channel and adjacent hillslopes over a 100 km distance. The floods increased the width of the active river channel by 54%. Subsequently, major landslides persisted for 15 months in at least nine locations for displacements > 2m. Among them, three moving hillslopes, ~80 km downstream from the Baige landslides, slumped more than 10 m one year after the floods. Extensive undercuts by the floods probably removed hillslope buttresses and triggered deformation response, suggesting a strong and dynamic channel-hillslope coupling. Our findings indicate that infrequent catastrophic outburst flooding plays an important role in landscape evolution. Persistent post-flood hillslope movement should be considered in disaster mitigation in high-relief mountainous regions.

1 Introduction

In eastern Tibet, the Jinsha, Mekong, and Salween - three of the largest Asian rivers - flow in parallel to each other and incise steep gorges, with up to 6 km of ridge-valley relief, while draining off the tectonically active margin of the Tibetan plateau (Larsen and Montgomery, 2012). The topographically varied terrain carved by fluvial incision, in association with the monsoonal climate, fosters a biodiversity hotspot with one of the highest speciation rates in the world (Myers et al., 2000). Ongoing rapid incision in the upper reach (e.g., Zhang et al., 2018) destabilizes hillslopes, leading to landslides, occasional river damming and associated landslide-lake outburst floods (LLFs) (e.g., Fan et al., 2020; Korup and Tweed, 2007). The extreme discharge of LLFs often entrain large volumes of sediments and are major drivers for geomorphic change. Yet, there is a lack of observations of the LLFs' catastrophic impacts on hillslopes (Baker, 2001; Turzewski et al., 2019), hindering the understanding of the geomorphic processes of LLFs and the development of hazards and landscape evolution models.

The extremely large flux of LLFs to the receiving rivers is the most obvious phenomenon and has significant social impacts (Dai et al., 2005; Delaney and Evans, 2015; Fan et al., 2012a; Ling and Evans, 2014; Wu et al., 2016). In addition, major LLFs often entrain many boulder size sediments from failed dams and along its routes (Cook et al., 2018a). Coarse-sediment

https://doi.org/10.5194/esurf-2021-14
Preprint. Discussion started: 11 March 2021

transport could cause much more significant bedrock incision and channel bank erosion than monsoon floods of similar magnitudes (Baynes et al., 2015; Larsen and Montgomery, 2012; Turzewski et al., 2019). Considering the frequency-magnitude relationship, LLFs could play a major role in shaping regional landscapes in the Himalayan orogens and other similar physiographic regions (Cook et al., 2018a).

Most of the geomorphic impacts of LLFs have been focused on their efficiency in sediment transportation and channel erosion (Cook et al., 2018a; Turzewski et al., 2019). Bank undercutting and parallel retreat are the most-frequently reported consequences of LLF's lateral erosion (Korup and Tweed, 2007). Landslides induced by bank undercutting and erosion along flood routes are often regarded as instantaneous impacts of LLFs by retrospective field reconnaissance or postevent image interpretations (Cook et al., 2018a; Higaki and Sato, 2012). Although such landslides often intersect with the LLF routes, they are usually bank collapses, and there is a lack of direct and persistent observations of LLFs' impacts on hillslope instability. In addition to these instantaneous landslides, LLFs may also disturb upper hillslopes adjacent to the collapsed banks over longer periods, which are more difficult to recognize and often overlooked.

Two landslides occurred on October 10, 2018, and November 10, 2018, near Baige along the Jinsha River. These successive landslides caused two mega floods (the peak discharge of the floods are ~10,000 and ~31,000 m^3/s, respectively) (Cai et al., 2020) in late October and late November 2018. In this study, the impacts of LLF on hillslope instability are investigated through quantitative measurements of downstream slope movements related to two upstream LLFs along the upper Jinsha River.

2 Materials and Methods

With an average elevation of 5 km above sea level and an area of ~ 2,500,000km^2, the Tibetan Plateau is the largest and highest orogen in the world by the collision between the Indian-Australian Plate and the Euro-Asian Plate. The rising grand plain altered the planetary wind system, and provides an arena among tectonics, climate, hydrologic and geomorphic processes. Among all parts of the plateau, the Southeast Tibetan Plateau is an ideal location to study interactions among tectonics, landscape evolution and climate change (Brookfield, 1998). Three major rivers, the Jinsha, Mekong, and Salween, cut through the plateau and flow in parallel in close distance of tens of kilometres from each other for over 300 km (Hallet and Molnar, 2001). In these deeply incised valleys, monsoonal precipitation compounds with active tectonics results in active mass wasting, an essential link between tectonic uplift and drainage efficiency in shaping the peculiar landscape of the eastern Tibet (Liu-Zeng et al., 2008; Zhang et al. 2021).

2.1 Two floods related to the Baige landslides in 2018

A slope near Baige village, Tibet Autonomous Region, China, failed twice in 2018 (Ouyang et al., 2019). The first landslide occurred on October 10, 2018, fully blocking the Jinsha River, forming a dammed lake with a maximum storage water of 0.29 km^3 (Fan et al., 2019). The lake started to drain naturally on October 12, 2018, leading to a first flood wave with a peak

https://doi.org/10.5194/esurf-2021-14
Preprint. Discussion started: 11 March 2021


Earth Surface Dynamics Discussions

discharge of 10,000m^3/s (Zhong et al., 2020). The first flood discharge finished on October 16, 2018 and there are no reports of economic damage during the first flood (Fan et al., 2019).

On November 3, 2018, the same slope collapsed again, leading to a second landslide dam, which fully blocked the Jinsha River. Since November 8, 2018, several excavators have been deployed to construct spillways. The lake started to drain through the spillway on November 12. The maximum water volume of the second lake was >0.52 km^3 (Fan et al., 2019). The second landslide lake caused a mega flood with a peak discharge of 31,000 m^3/s near Baige (Zhong et al., 2020). This flood caused significant damages to major roads, schools, buildings and farms in the Diqing and Lijiang Prefectures, Yunnan Province, ~ 500 km downstream of the Baige landslides. Fortunately, no casualties were reported during these two LLFs due to effective and timely evacuations.

Hillslopes on both sides along the Jinsha River were investigated for the downstream 100 km-long stretch from the Baige landslide (Fig. 1). The elevation of the region ranges from 2,500 m to 5,400 m, with a mean value of 4,100 m above sea level (*als.*). In the study reach, the Jinsha River cut through the Plateau and flows from north to south; the valley floor descends from 2,900 m *asl.* to 2,600 m *asl*. (Fig. 1) over ~ 80 km distance.

2.2 Slope displacements derived from the Sentinel-2 images

We used the coregistration of optically sensed images and correlation (COSI-Corr) method to derive subpixel horizontal slope deformation in Sentinel-2 image pairs (Leprince et al., 2007). An image pair in the COSI-Corr includes a reference image and a target image. Using the reference image from the earlier time, ground deformation can be derived from the target image in the later time. To detect slope deformation before and after the Baige floods, we used an image pair on November 13, 2015, and November 12, 2018, and a second image pair on November 12, 2018, and November 12, 2019. Images in these two pairs cover a large area from the Baige landslide to a 100 km downstream region along both banks of the Jinsha River (Fig. 1). Both image pairs are from the same date of different years to minimize uncertainties by having similar solar zenith/azimuth angles (Yang et al., 2020, Yang et al., 2020a).

We further analysed the Mindu section, ~80 km from the Baige landslide, where more moving hillslopes were detected. In this section, we composed 16 image pairs to detect the time series of slope displacements after the Baige floods. The dates of the reference and target images in these 16 image pairs are shown in Table 1. In this work, four reference images in January (3rd, 13rd, 16th) and February (12nd) 2017 are used. Acquisition dates of these reference images are very close to ensure no displacements occur among them, because slopes in this section are stable before October 2018 and have been moving since then (Fig. 2). We used the same stable zone near Mindu to correct the image shifts between the reference and the target images with Yang et al. (2020b). In addition, we used two Sentinel-2 images in the summer months of July 15, 2017, and August 16, 2019, to map the width of the active channel before and after the 2018 floods.

https://doi.org/10.5194/esurf-2021-14
Preprint. Discussion started: 11 March 2021


Earth Surface Dynamics Discussions
Open Access
EGU

3 Results

3.1 Post-flood slope movements along the Jinsha River

We identified at least nine post-flood moving slopes (Fig. 2) in the studied reach. Before the Baige floods in 2018 (2015.11-2018.11), very few slopes along the Jinsha River had displacements larger than 2 m, whereas there were widespread slope movement with displacements larger than 2 m near the riverbank after the floods (2018.11-2019.11). All these newly emerged slope movements had larger deformations near the valley bottom and decreased progressively higher up along the hillslopes.

Near the Mindu village, ~80 km from the Baige landslide, at least four hillslopes are slipping (d2 in Fig. 2). We showed displacements of these slopes in ten target images from January 13, 2018 to February 7, 2020 (Fig. 3) relative to the base images in early 2017 (Table 1). No displacements (> 2 m) were detected in the MD-1 (MD is short for the village Mindu), MD-2 and MD-4 hillslopes before the floods until late October and November 2018 (Fig. 3 a-b). The toes of these hillslopes began to deform after the floods (since November 29, 2018, Fig. 3 c-g). The deformation started from riverbanks and became larger with time and propagated upslope until the end of the study period (February 2020, Fig. 3 g-j). At the MD-3 area, the hillslope deformation was less than 4 m from January 2017 to January 2018 (Fig. 3a), and less than 8 m by November 9, 2018 (Fig. 3c); however, an acceleration could be observed from November 2018 to January 2019 (Fig. 3 d-e). There are some background noises on hillslopes and tributary catchments in Fig. 3, which is irrelevant to the 2018 floods.

We further selected three representative points, each on the MD-1, MD-2 and MD-3 landslides, respectively, and measured their cumulative movements and velocity at 16 different dates (Table 1) from January 2018 to February 2020 (Fig. 4). The points on MD-1 and MD-2 landslides show similar temporal patterns. Movement for both points before November 2018 is minimal (< 0.18 cm/d from February 2017) compared to 4.55 cm/d from November 2018 to April 2019. Cumulative displacements at the MD-1 and MD-2 points continued to increase from ~8 m to ~ 12 m since then. Significant acceleration of the slope movement was also found for the point on MD-3 landslide. The MD-3 point moved 1.52 cm/d (uncertainty <0.26 cm/d) before November 9, 2018, and then increased to 4.84 cm/d (uncertainty <0.96 cm/d) from November 2018 to February 2019. No additional displacements were detected after February 2019, which is due to collapse of the slope at the point.

3.2 Concurrent landslides and channel expansion during the 2018 floods

Active channel width increased for almost all parts of the study area (Fig. 5). There was widespread lateral erosion of the Jinsha River bank in the form of riverbank undercutting and parallel retreat. The successive LLFs increased the mean width of the active channel from 96.33 +/- 10 m to 148.56 +/- 10 m. The river width expanded 52.2 m on average after the 2018 floods. Lateral erosion to the Jinsha riverbanks led to undercutting of slopes, which propagated up hillslope and could have been the direct trigger for the expansion of landslides existing before the Baige LLFs. In addition, we observed a few new landslides (Fig. 6), which could also be concurrent with the 2018 LLFs. We further measured the area of these concurrent

https://doi.org/10.5194/esurf-2021-14
Preprint. Discussion started: 11 March 2021

landslides and postevent moving slopes with deformation >2 m in January 2020. The areas of these concurrent landslides and moving slopes were 2.18×10^5 m^2 and 11.86×10^5 m^2, respectively. The areal extent of the moving slopes (with deformation > 2 m) was 5.4 times that of the concurrent landslides. Most of these moving slopes and the concurrent landslides occurred in the reach that experienced significant increase in river channel width.

The influence of the 2018 floods on adjacent hillslopes could be larger than reported here. In this work, the method we use can reliably track slope deformation >2 m (Stumpf et al., 2017; Yang, 2020) and we only monitored the downstream riverbanks for less than 2 years. It is possible that there could be more slow-moving slopes with cumulative displacements <2 m but not detected by our method.

4 Discussion

4.1 Magnitudes of the 2018 Baige LLFs

The nearest downstream hydrological station is the Batang station, which is 190 km away from the Baige landslide. The multi-year average discharge measured at the station is 924 m^3/s (Xiong et al., 2020). The recorded peak discharges at this station for the first and the second Baige floods are 7,850 m^3/s and 21,200 m^3/s, respectively. We collected 40-year records of annual peak discharges for the Batang station from 1953 to 2017 representing background climatic discharges (Fig. 7). Peak discharges caused by the Baige floods are 1.3 and 3.6 times larger than the recorded maximum annual peak discharge in 1954 (Duan et al., 2016). In addition, measured suspended sediment discharge for the first and second Baige floods are 2.3 and 4.5 times larger than the maximum annual peak sediment discharge (9.33 kg/m^3 in 1972), respectively.

Although the peak discharge of LLFs would decrease as it propagates downstream (Cook et al., 2018; Schwanghart et al., 2016; Cenderelli et al., 2001), the discharges recorded 190 km downstream the Baige landslide are still much higher than background climate values. This means that peak discharges would be much larger than normal climate discharges in the river section between the Baige landslide and the Batang station during these two floods. These exceptionally high discharges with record-high sediments would be much more efficient to erode river channels.

4.2 Implications for mountain hazards

Outbursts of landslide lakes present severe flooding threats to downstream communities (Delaney and Evans, 2015; Ling and Evans, 2014; Dai et al., 2005; Fan et al., 2012a). Landslide dams can be formed at more diverse locations along the river (Liu et al., 2019) than other types of natural dams, such as glacier or moraine dams, which are usually located in highlands near riverheads and are far from human communities (Cook et al., 2018). Therefore, LLFs pose more serious threats to humans due to their closer distances to densely populated regions.

The observations in this study show that the 2018 Baige landslides destabilized some major downstream hillslopes tens of hundreds of kilometres away. If these hillslopes fail subsequently, they may cause further disruptions to the main channel, forming a domino effect of “landslide-LLF-landslide” hazard chains. This possible process demonstrates the propagation of

https://doi.org/10.5194/esurf-2021-14
Preprint. Discussion started: 11 March 2021

LLF hazards downstream, which has not been given enough attention in the past, but should be considered in future disaster mitigation measures. The findings of this work also have important implications for the ongoing construction of the Sichuan-Tibet railway, which runs through deepest gorges along the Jinsha, Mekong, and Salween Rivers.

4.3 Possible mechanism for downstream erosion

The eastern Tibetan Plateau is tectonically active and influenced by the Asian monsoon with intense storms in the summer months (Cook et al., 2018b). Active faults, shear zones and sutures subparallel to the trunk rivers shatter the rock, make them susceptible to cracking thus result in relatively high erodibility (Liu-Zeng et al. 2008). We examined all moving slopes in the Mindu reach and found that most of these slopes had tensile cracks and surface disruptions before the Baige landslides (Fig. 8). Strong seismicity could cause intense regional erosion by triggering numerous landslides and resulting in unstable strata (Hovius et al., 2011; Li et al., 2017; Parker et al., 2011).

It is possible that weak strata from historic strong earthquakes or extreme precipitation along the studied reach were activated by the 2018 LLFs' lateral erosion. The sudden draining of a landslide lake can release a large volume of water, dramatically raise the downstream discharge and entrain large volumes of sediments along its routes and cause extensive erosion to river channels (Baynes et al., 2015; Cook et al., 2018a; Higali et al., 2012; Li et al., 2020; Turzewski et al., 2019). The removal of buttressing by the 2018 LLFs' erosion may attribute to the moving hillslopes in downstream reaches, which is substantiated by our observation that detected deformations are larger near the riverbank and decrease in concentric ellipses upslope.

4.4 Implications for geomorphic processes

Previous works about the influence of LLFs on hillslope instability along major rivers are hypothetical and lack direct observations (Cook et al., 2018a; Higaki and Sato, 2012). Our findings are proofs to the theory that landsliding in fluvial systems is a key component to link climate and tectonics in landscape evolution (Larsen and Montgomery, 2012; Brookfield 1998). Mega-floods can cause both instant landslides in terms of bank collapses (Cook et al., 2018) and post-flood landslides by destabilizing hillslopes along fluvial channels that fail in later years. However, much focus has been placed on the immediate hazards of LLF such as the instantaneous downstream floods and inundations (Dai et al., 2005; Delaney et al., 2015; Fan et al., 2012a). The lack of observations on post-flood landslides hinders our understanding on the long term impacts of mega floods to landslides, landscape evolution and related risks. This work shows that in addition to immediate (or concurrent) landslides (Cook et al., 2018a; Higaki and Sato, 2012), the impact of LLF lateral erosion could propagate uphill by disturbing adjacent hillslope stability for a prolonged period, illustrating the dynamic response of mountain hillslopes to channel incision.

Infrequent catastrophic floods could play an important role in landscape evolution (Cook et al., 2018a). The active channel width before the Baige floods mirrors the background climate maximum runoff to lateral erosion. Our finding that the mean active channel width increased by 54.2% after the LLFs in 2018 indicate that such rare catastrophic events could leave a

https://doi.org/10.5194/esurf-2021-14
Preprint. Discussion started: 11 March 2021

disproportionate footprint on local landscapes. Recent progress confirmed that bedrock canyons on the surfaces of Mars and Earth are probably caused by infrequent catastrophic floods instead of uniform, steady erosion from background runoff (Keisling et al., 2020; Larsen and Lamb, 2016; Malatesta et al., 2017).

However, quantitative assessment of the role of LLFs on the long-term landscape evolution awaits for future research. First, the relationship between the magnitude and frequency of LLFs should be constrained. The volume of impoundment water and downstream channel morphology, which is site specific, determines the severity/magnitude of an LLF (Fan et al., 2012b). Landslide triggers, such as large-magnitude earthquakes and high-intensity storms, control the frequency of LLFs (Liu et al., 2019). Strong earthquakes can trigger numerous landslides within river systems and form many landslide-dammed lakes (Fan et al., 2012b), the outbursts of which could accelerate the flush of postseismic landslide debris (Croissant et al., 2017). In addition, the strength of hillslopes along the LLF pathway should also be constrained. Hillslopes composed of weaker bedrock or repeatedly damaged by seismicity could have more slope erosions after the occurrence of LLFs. Despite these related but poorly understood questions, our observations indicate that LLFs could significantly improve the efficiency of regional erosion and can be an important internal variable that modulates regional erosion.

5 Conclusions

In October and November 2018, two large landslides occurred on the same slope near the Baige village along the Jinsha River, leading to two successive LLFs downstream. Besides three new landslides and widespread lateral erosion, we found the LLFs destabilized at least nine hillslopes, which progressively deformed over the following year within a hundred kilometres downstream of the landslide. Bank undercutting and parallel retreat are prevalent after the Baige floods, which probably activated these slopes by removing their buttresses. Landslide hazards propagate to long-range downstream regions by releasing mega floods to undercut hillslopes along river channels, leading to more destabilized hillslopes. Persistent monitoring of slope deformation along major rivers may be a viable way to detect possible hazards in remote mountain regions.

Compared to LLF-triggered concurrent landslides, subsequent slowly moving slopes are less easily recognized and thus often overlooked. Realizing that LLFs may lead to more hillslope slumping, in larger areal extent, and during the prolonged period afterwards could help researchers to obtain a holistic picture of LLFs' impacts and improve geomorphic models of landscape evolution. In the future, LLF contributions to hillslope erosion may be constrained by quantifying the magnitude-frequency relationship.

Data availability

The Sentinel-2 remote sensing data can be accessed from the Sentinel-hub (https://www.sentinel-hub.com/). The ALOS World 3D-30m DEM are available on the JAXA website (https://www.eorc.jaxa.jp/ALOS/en/aw3d30/index.htm).

https://doi.org/10.5194/esurf-2021-14
Preprint. Discussion started: 11 March 2021

Author contributions

The manuscript was written by WY with major contribution by JF and JLZ. WY processed the data. WY, JF and JLZ interpreted the results. All authors reviewed and approved the manuscript.

Competing interests

The authors declare that they have no conflict of interest.

Acknowledgments

Sentinel-2 images are courtesy of the ESA. We acknowledge the JAXA for the use of the ALOS World 3D-30m DEM. We thank the CIT team for the use of the COSI-Corr.

Financial support

The Second Tibetan Plateau Scientific Expedition and Research Program (STEP, Grant No. 2019QZKK0906) and the National Science Foundation of China (No. 41807500) jointly support this work.

References

Baker, V. R.: Water and the Martian landscape. Nature, 412(6843), 228-236, 2001.

Baynes, E. R. C., Attal, M., Dugmore, A. J., Kirstein, L. A., and Whaler, K. A.: Catastrophic impact of extreme flood events on the morphology and evolution of the lower Jökulsá á Fjöllum (northeast Iceland) during the Holocene. Geomorphology, 250, 422-436, 2015.

Brookfield, M. E.: The evolution of the great river systems of southern Asia during the Cenozoic India --Asia collision: rivers draining southwards. Geomorphology, 22, 285-312, 1998.

Cenderelli, D. A. and Wohl, E. E.: Peak discharge estimates of glacial-lake outburst floods and "normal" climatic floods in the Mount Everest region, Nepal. Geomorphology, 40(1-2), 57-90, 2001.

Cai, Y., Cheng, H., Wu, S., Yang, Q., Wang, L., Luan Y., and Chen, Z.: Breaches of the Baige Barrier Lake: Emergency response and dam breach flood. Sci. China Technol. Sci., 63(7), 1164-1176, 2020.

Cook, K. L., Andermann, C., Gimbert, F., Adhikari, B. R., and Hovius, N.: Glacial lake outburst floods as drivers of fluvial erosion in the Himalaya. Science, 362(6410), 53, 2018a.

Cook, K. L., Hovius, N., Wittmann, H., Heimsath, A. M., and Lee, Y.: Causes of rapid uplift and exceptional topography of Gongga Shan on the eastern margin of the Tibetan Plateau. Earth Planet Sc. Lett., 481, 328-337, 2018b.

https://doi.org/10.5194/esurf-2021-14
Preprint. Discussion started: 11 March 2021

Croissant, T., Lague, D., Steer, P., and Davy, P.: Rapid post-seismic landslide evacuation boosted by dynamic river width. Nat. Geosci., 10, 680–684, 2017.

Dai, F. C., Lee, C. F., Deng, J. H., and Tham, L. G.: The 1786 earthquake-triggered landslide dam and subsequent dam-break flood on the Dadu River, southwestern China. Geomorphology, 65(3), 205-221, 2005.

Delaney, K. B. and Evans, S. G.: The 2000 Yigong landslide (Tibetan Plateau), rockslide-dammed lake and outburst flood: Review, remote sensing analysis, and process modelling. Geomorphology, 246, 377-393, 2015.

Duan, W., He, B., Nover, D., Fan, J., Yang, G., Chen, W., Meng, H., and Liu, C.: Floods and associated socioeconomic damages in China over the last century. Nat. Hazards, 82, 401-413, 2016.

Fan, X., Dufresne, A., Siva Subramanian, S., Strom, A., Hermanns, R., Tacconi Stefanelli, C., Hewitt, K., Yunus, A.P., Dunning, S., Capra, L., Geertsema, M., Miller, B., Casagli, N., Jansen, J.D., and Xu, Q.: The formation and impact of landslide dams – State of the art. Earth-Sci. Rev., 203, 103116, 2020.

Fan, X., Tang, C., van Westen, C., and Alkema, D.: Simulating dam-breach flood scenarios of the Tangjiashan landslide dam induced by the Wenchuan Earthquake. Nat. Hazard Earth Sys., 12(10), 3031-3044, 2012a.

Fan, X., van Westen, C. J., Xu, Q., Gorum, T., and Dai, F.: Analysis of landslide dams induced by the 2008 Wenchuan earthquake. J. Asian Earth Sci., 57, 25-37, 2012b.

Fan, X., Xu, Q., Alonso-Rodriguez, A., Subramanian, S. S., Li, W., Zheng, G., Dong, X., and Huang, R.: Successive landsliding and damming of the Jinsha River in eastern Tibet, China: prime investigation, early warning, and emergency response. Landslides, 16(5), 1003-1020, 2019.

Hallet, B. and Molnar, P.: Distorted drainage basins as markers of crustal strain east of the Himalaya. J. Geophys. Res., 106(B7), 13697-13709, 2001.

Higaki, D. and Sato, G.: Erosion and sedimentation caused by glacial lake outburst floods in the Nepal and Bhutan Himalayas. Global Environ. Res., 16(1), 71-76, 2012.

Hovius, N., Meunier, P., Lin, C., Chen, H., Chen, Y., Dadson, S., Dadson, S., Hong, M., and Lines, M.: Prolonged seismically induced erosion and the mass balance of a large earthquake. Earth Planet Sc. Lett., 304(3–4), 347-355, 2011.

Keisling, B. A., Nielsen, L. T., Hvidberg, C. S., Nuterman, R., and DeConto, R. M.: Pliocene–Pleistocene megafloods as a mechanism for Greenlandic megacanyon formation. Geology, 48(7), 737-741, 2020.

Korup, O. and Tweed, F. Ice, moraine, and landslide dams in mountainous terrain. Quaternary Sci. Rev., 26(25-28), 3406-3422, 2007.

Larsen, I.J. and Lamb, M.P. Progressive incision of the Channeled Scablands by outburst floods. Nature 538:229-232, 2016.

Larsen, I. J. and Montgomery, D. R.: Landslide erosion coupled to tectonics and river incision. Nat. Geosci., 5(7), 468-473, 2012.

Leprince, S., Barbot, S., Ayoub, F., and Avouac, J.: Automatic and precise orthorectification, coregistration, and subpixel correlation of satellite images, application to ground deformation measurements. IEEE T. Geosci. Remote, 45 (6), 1529-1558, 2007.

https://doi.org/10.5194/esurf-2021-14
Preprint. Discussion started: 11 March 2021

Li, G., West, A. J., Densmore, A. L., Jin, Z., Zhang, F., Wang, J., Clark, M., and Hilton, R.G.: Earthquakes drive focused denudation along a tectonically active mountain front. Earth Planet Sc. Lett., 472, 253-265, 2017.

Li, T., Fuller, T. K., Sklar, L. S., Gran, K. B., and Venditti, J. G.: A Mechanistic Model for Lateral Erosion of Bedrock Channel Banks by Bedload Particle Impacts. J. Geophys. Res-Earth, 125(6), e2019JF005509, 2020.

Ling, S. and Evans S. G.: GIS-based analysis of 1933 Diexi Landslides and dam breach on the Min River, Sichuan, China, paper presented at EGU General Assembly Conference Abstracts, 2014.

Liu, W., Carling, P. A., Hu, K., Wang, H., Zhou, Z., Zhou, L, Liu, D., Lai, Z., and Zhang, X.: Outburst floods in China: A review. Earth-Sci. Rev., 197, 102895, 2019.

Liu-Zeng, J., Tapponnier, P., Gaudemer, Y., and Ding, L.: Quantifying landscape differences across the Tibetan plateau: Implications for topographic relief evolution. J. Geophys. Res-Earth, 113(F4), F04018, 2008.

Malatesta, L. C., Prancevic, J. P., and Avouac, J. P.: Autogenic entrenchment patterns and terraces due to coupling with lateral erosion in incising alluvial channels. J. Geophys. Res-Earth, 122(1), 335-355, 2017.

Myers, N., Mittermeier, R. A., Mittermeier, C. G., da Fonseca, G. A. B., and Kent, J.: Biodiversity hotspots for conservation priorities. Nature, 403, 853-858, 2000.

Ouyang, C., An, H., Zhou, S., Wang, Z., Su, P., Wang, D., Chen, D., and She, J.: Insights from the failure and dynamic characteristics of two sequential landslides at Baige village along the Jinsha River, China. Landslides, 16, 1397-1414, 2019.

Parker, R. N., Densmore, A. L., Rosser, N. J., De Michele, M., Li, Y., Huang, R., Whadcoat S., and Petley, D.N.: Mass wasting triggered by the 2008 Wenchuan earthquake is greater than orogenic growth. Nat. Geosci., 4(7), 449-452, 2011.

Schwanghart, W., Worni, R., Huggel, C., Stoffel, M., and Korup, O.: Uncertainty in the Himalayan energy–water nexus: estimating regional exposure to glacial lake outburst floods. Environ. Res. Lett., 11(7), 074005, 2016.

Stumpf, A., Malet, J. P., and Delacourt, C.: Correlation of satellite image time-series for the detection and monitoring of slow-moving landslides. Remote Sens. Environ., 189, 40-55, 2017.

Turzewski, M. D., Huntington, K. W., and LeVeque, R. J.: The Geomorphic Impact of Outburst Floods: Integrating Observations and Numerical Simulations of the 2000 Yigong Flood, Eastern Himalaya. J. Geophys. Res-Earth, 124(5), 1056-1079, 2019.

Wu, Q., Zhao, Z., Liu, L., Granger, D.E., Wang, H., Cohen, D.J., Wu, X., Ye, M., Bar-Yosef, O., Lu, B., Zhang, J., Zhang, P., Yuan, D., Qi, W., Cai, L., and Bai, S.: Outburst flood at 1920 BCE supports historicity of China's Great Flood and the Xia dynasty. Science, 353(6299), 579, 2016.

Xiong, M., Li, J., and Chen, Y.: Runoff Trend and Natural Driving Force in the Upper Jinsha River. J. Water Resour. Res., 9(3), 235- 248, 2020.

Yang, W.: Selecting the best image pairs to measure slope deformation. Sensors, 20(17), 4721, 2020.

Yang, W., Wang, Y., Wang, Y., Ma, C., and Ma, Y.: Retrospective deformation of the Baige landslide using optical remote sensing images. Landslides, 17(3), 659-668, 2020a.

https://doi.org/10.5194/esurf-2021-14
Preprint. Discussion started: 11 March 2021

Yang, W., Liu, L., and Shi, P.: Deriving slope movements for an imminent landslide along the Jinsha river. Nat. Hazard Earth Sys., 20, 3215-3224, 2020b.

Zhang, H., Kirby, E., Pitlick, J., Anderson, R.S., and Zhang, P.: Characterizing the transient geomorphic response to base-level fall in the northeastern Tibetan Plateau. J. Geophys. Res-Earth, 122(2), 546-572, 2017.

Zhang, J., Yang, H., Liu-Zeng, J., Ge, Y., Wang, W., Yao, W., and Xu, S.: Reconstructing the incision of the Lancang River (Upper Mekong) in southeastern Tibet below its prominent knickzone using fluvial terraces and transient tributary profiles. Geomorphology, 376, 107551, 2021.

Zhong, Q., Chen, S., Wang, L., and Shan, Y.: Back analysis of breaching process of Baige landslide dam. J. Hydrol., 17, 1681-1692, 2020.

https://doi.org/10.5194/esurf-2021-14
Preprint. Discussion started: 11 March 2021

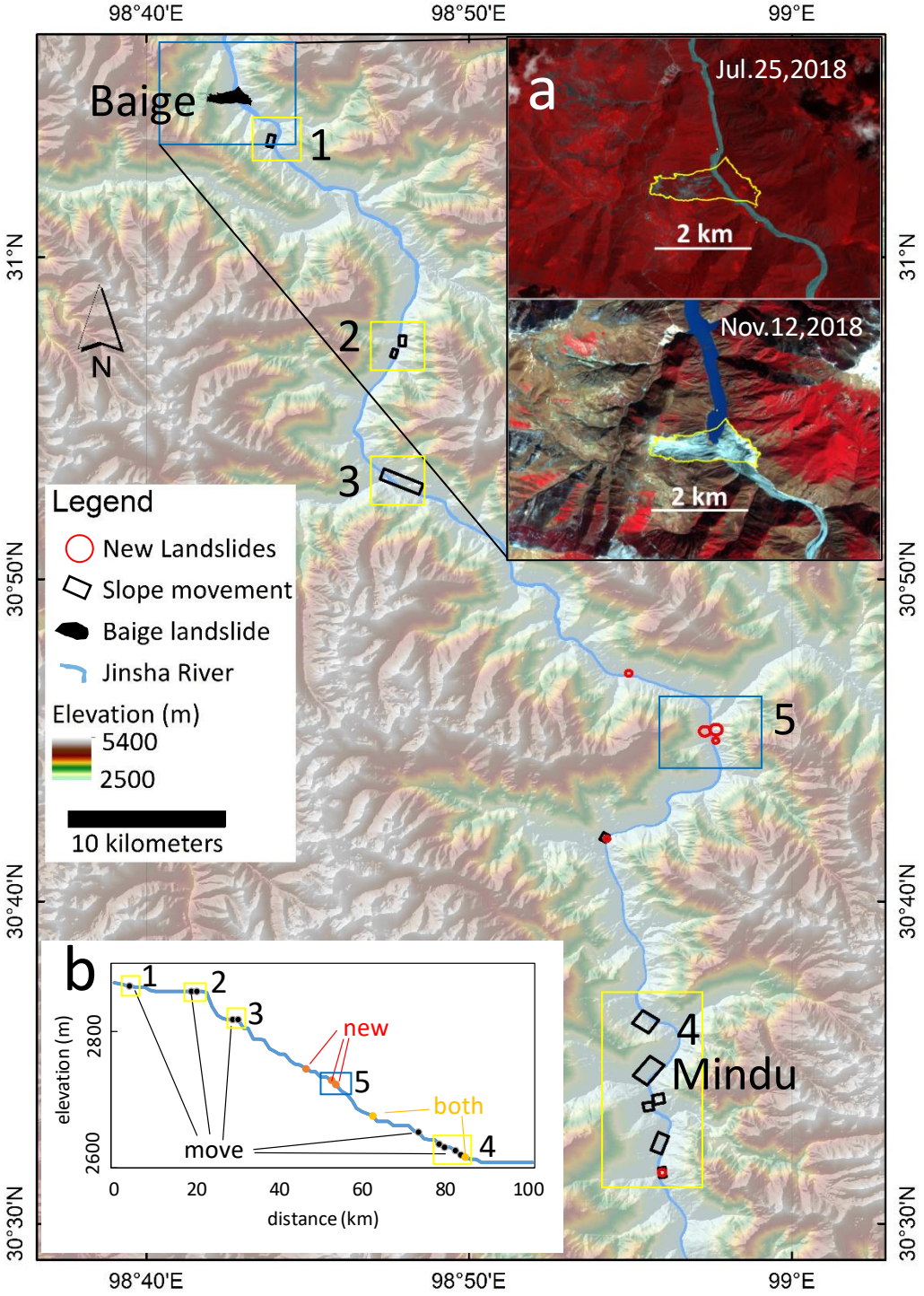

Figure 1: Map of the Jinsha River study region. Black rectangles are moving slopes detected after the Baige floods. Red circles are new landslides after the floods. Yellow rectangles with black numbers 1 to 4 are subregions in Figure 2. Blue rectangles with black numbers 5-6 are subregions in Figure 3. (A) Two Sentinel-2 images were taken before the Baige landslide in July 2018 (top) and

https://doi.org/10.5194/esurf-2021-14
Preprint. Discussion started: 11 March 2021

Earth Surface Dynamics Discussions
Open Access
EGU

after in November 2018 (bottom). (B) Longitudinal profile of the Jinsha River in this section from the ALOS World 3D-30m DEM, and the localities of new landslides and moving slopes are marked. The Jinsha River is digitized by the authors from Sentinel-2 images before the 2018 floods.

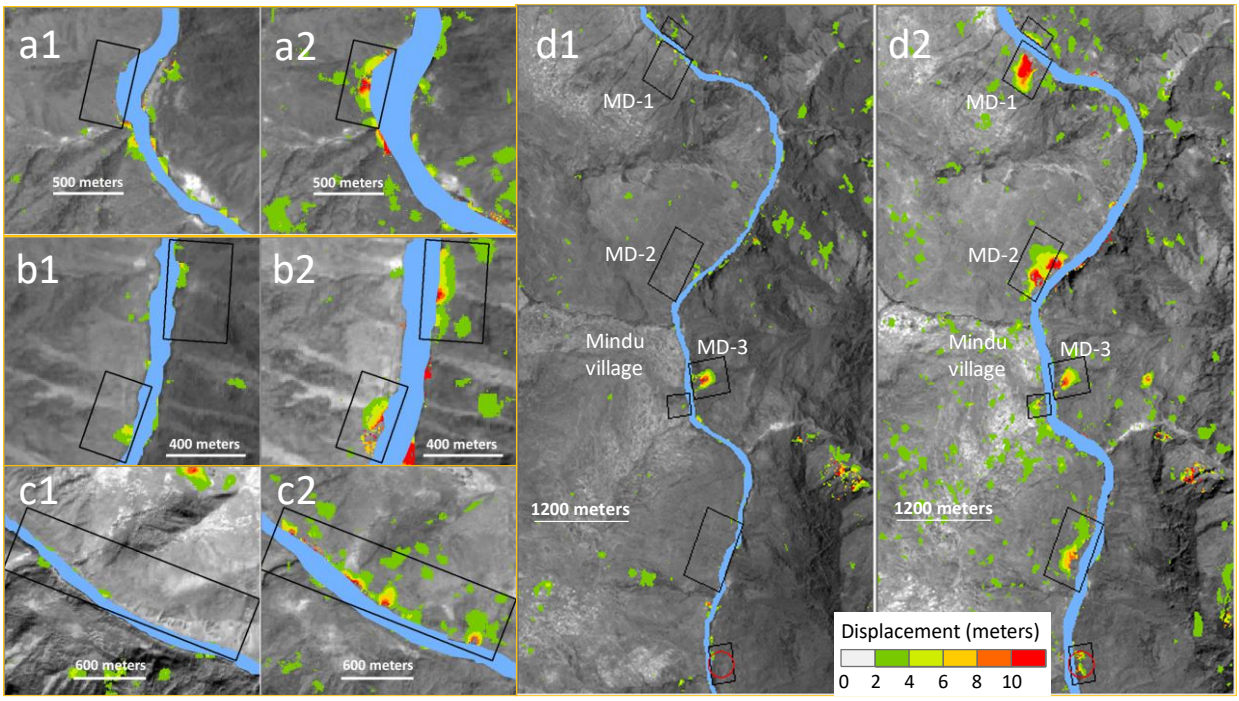

Figure 2. Moving slopes in four selected sections along the Jinsha River (a-d) before (2015.11-2018.11) and after (2018.11-2019.11) the Baige floods. Left subplots (a1, b1, c1, d1) are preflood results and right subplots (a2, b2, c2, d2) are postflood results. MD is short for the village Mindu. Background images are cloud-free grey scale Sentinel-2 images before and after the 2018 floods.

https://doi.org/10.5194/esurf-2021-14
Preprint. Discussion started: 11 March 2021

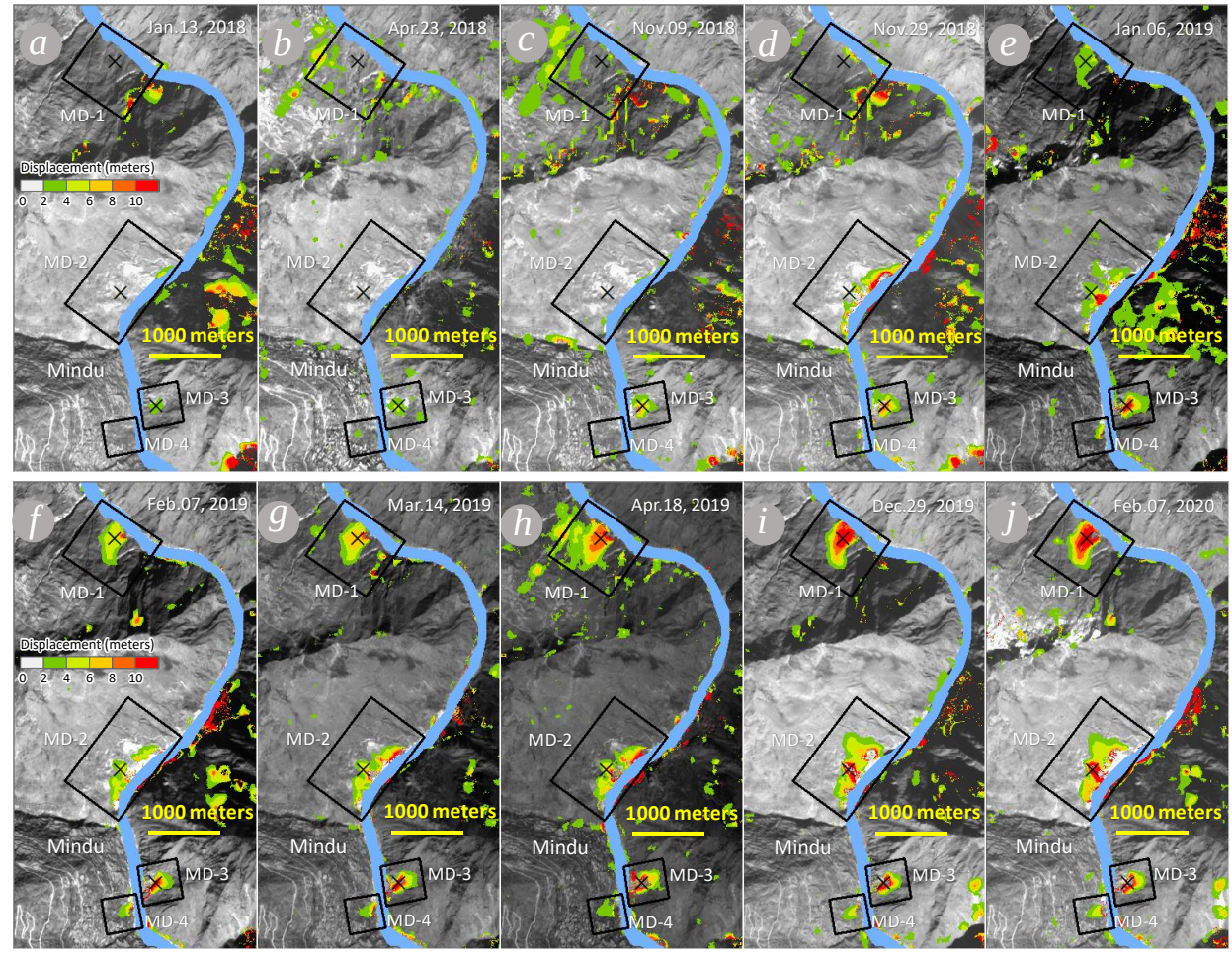

Figure 3. Cumulative hillslope displacements near the Mindu village at different times between early 2018 and early 2020, using the early 2017 image (either January or February) as the reference. Cumulative displacement (a-b) before the first Baige flood, (c) between the two floods, and (d-j) at different times between November 29, 2019 and February 07, 2020. Background images are also respective target Sentinel-2 images of the ending date for the calculation.

https://doi.org/10.5194/esurf-2021-14
Preprint. Discussion started: 11 March 2021

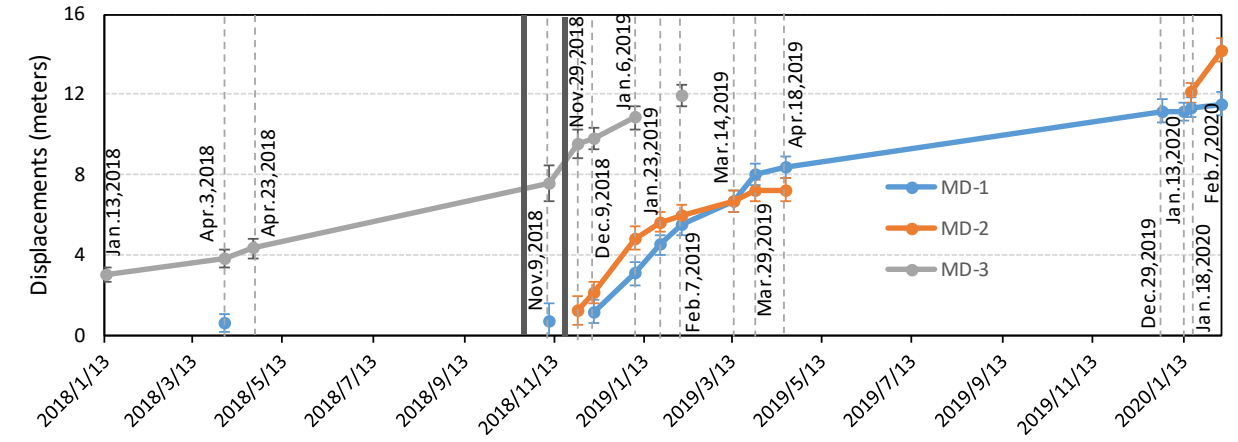

Figure 4. Cumulative displacements of three points (crosses in Figure 3) on three slopes near Mindu village (Two black vertical lines indicate the occurrence date of the Baige outburst floods in late October and November 2018).

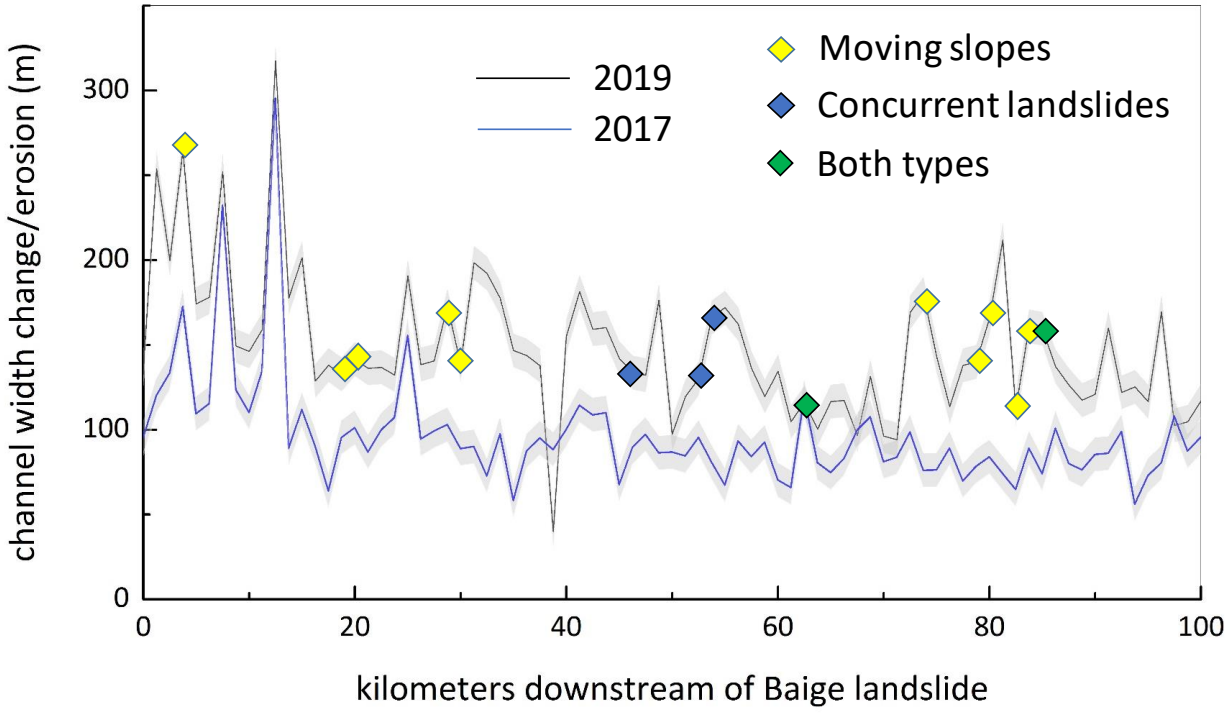

340

Figure 5. River widths before and after the Baige floods. The gray shadow indicates an uncertainty of ±1 pixel in the Sentinel-2 imagery.

https://doi.org/10.5194/esurf-2021-14
Preprint. Discussion started: 11 March 2021

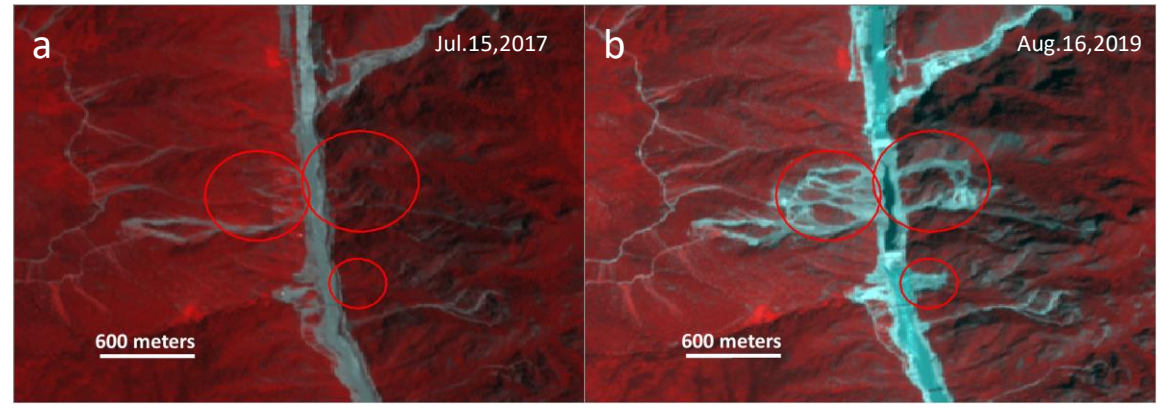

345 **Figure 6. Concurrent landslides related to the Baige floods. False composite Sentinel-2 images are acquired on July 15, 2017 (a) and August 16, 2019 (b). The spatial extent of this area is shown as the rectangle 5 in Figure 1.**

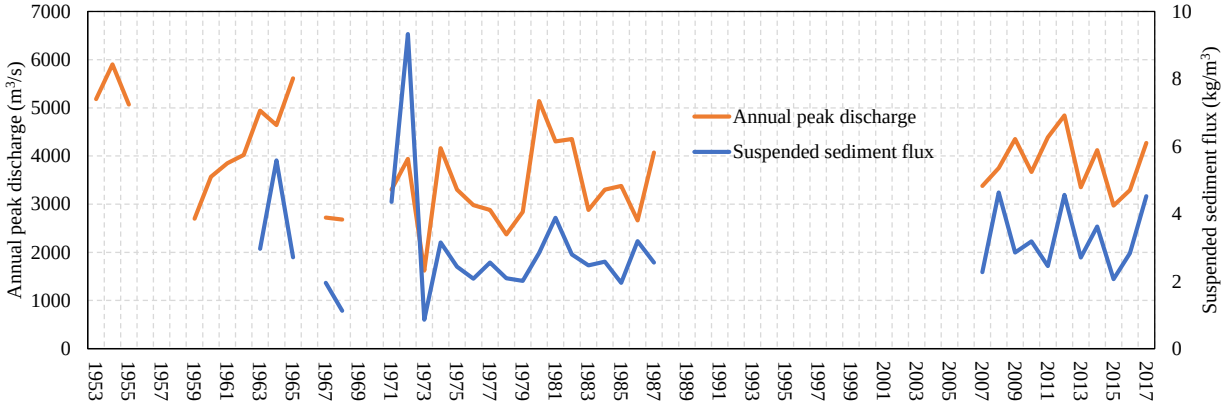

Figure 7. Multi-year peak discharge and suspended sediment flux at the Batang station. Note the discharges for the 2018 Baige floods are 7,850 m3/s and 21,200 m3/s, respectively. The suspended sediment flux are 21.6 kg/m3 and 42 kg/m3, respectively.

https://doi.org/10.5194/esurf-2021-14
Preprint. Discussion started: 11 March 2021

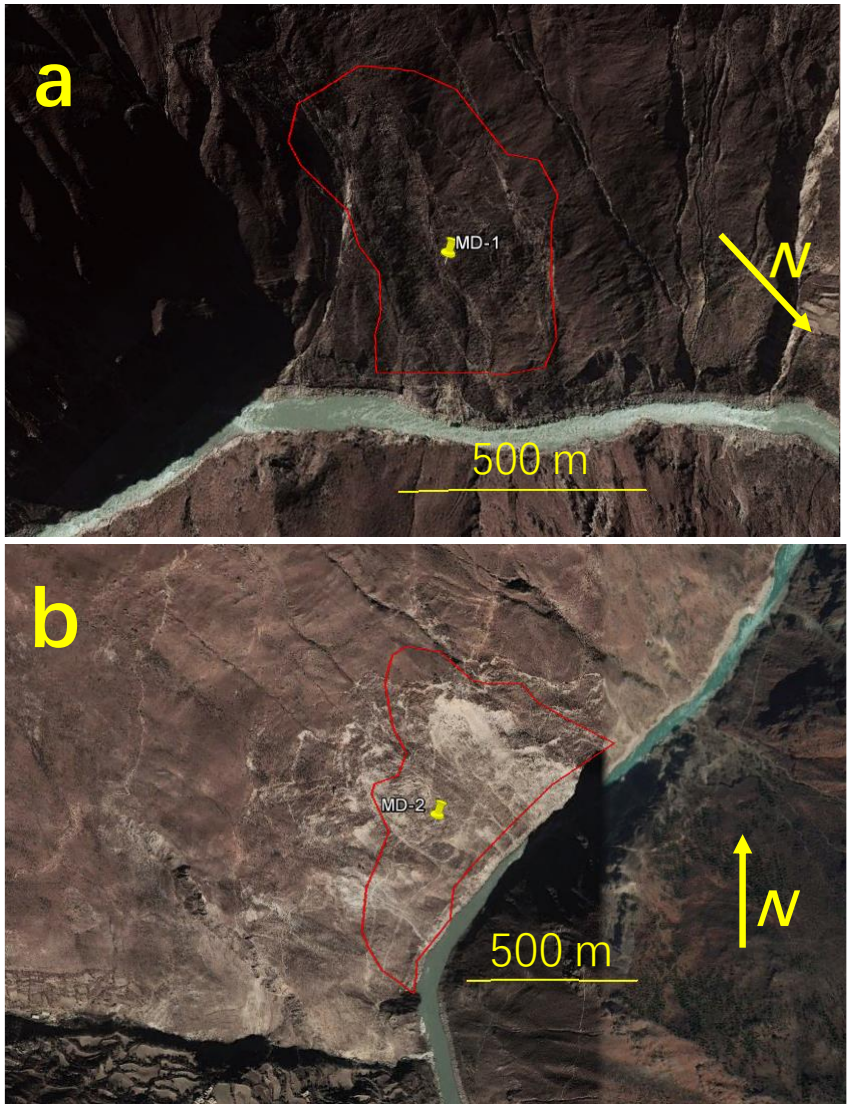

350

https://doi.org/10.5194/esurf-2021-14
Preprint. Discussion started: 11 March 2021

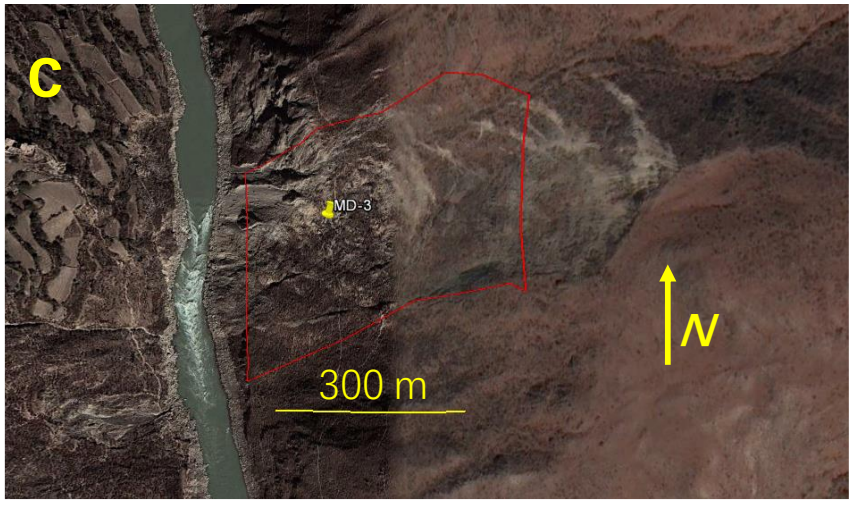

Figure 8. Tensile cracks of major hillslopes before the 2018 Baige floods as seen from high-spatial-resolution images from © Google Earth.

355 **Table 1. Dates of images used in the Mindu section. Image pairs with grey background are shown in Figure 3. All image pairs are used in Figure 4.**

Image pairs	Reference images	Target images
#1	Jan. 03, 2017	Jan. 13, 2018
#2	Feb. 12, 2017	Apr. 03, 2018
#3	Feb. 12, 2017	Apr. 23, 2018
#4	Jan. 03, 2017	Nov. 09, 2018
#5	Jan. 03, 2017	Nov. 29, 2018
#6	Jan. 03, 2017	Dec. 09, 2018
#7	Jan. 16, 2017	Jan. 06, 2019
#8	Feb. 12, 2017	Jan. 23, 2019
#9	Feb. 12, 2017	Feb. 07, 2019
#10	Feb. 12, 2017	Mar. 14, 2019
#11	Feb. 12, 2017	Mar. 29, 2019

https://doi.org/10.5194/esurf-2021-14
Preprint. Discussion started: 11 March 2021

Earth Surface Dynamics Discussions
Open Access
EGU

#12	Feb. 12, 2017	Apr. 18, 2019
#13	Jan. 03, 2017	Dec. 29, 2019
#14	Jan. 13, 2020	Jan. 13, 2020
#15	Feb. 12, 2017	Jan. 18, 2020
#16	Feb. 12, 2017	Feb. 07, 2020